Journal of Urban and Environmental Engineering, v.11, n.1, p.30-41

ISSN 1982-3932
doi: 10.4090/juee.2017.v11n1.030041

Journal of Urban and Environmental Engineering

www.journal-uee.org

UPGRADING OF MOROCCAN OLIVE MILL WASTEWATER USING ELECTROCOAGULATION: KINETIC STUDY AND PROCESS PERFORMANCE EVALUATION

Reda Elkacmi[1*], Noureddine Kamil[2] and Mounir Bennajah[3]

[1]Département Chimie et Valorisation (CV), Faculté des sciences Ain-Chock, Université Hassan II de Casablanca, BP 5366 Maarif, Casablanca, Morocco
[2]Laboratoire de Mécanique Productique & Génie Industriel (LMPGI), Université Hassan II Ain Chock, Ecole Supérieure de Technologie, Km 7 Route El Jadida, Casablanca, Morocco, Morocco
[3]Département Génie des Procédés, Ecole Nationale Supérieure des Mines de Rabat (ENSMR), BP 753 Agdal, Rabat, Morocco, Morocco

Received 2 November 2016; received in revised form 13 February 2017; accepted 11 March 2017

Abstract: Treatment of olive mill wastewater (OMW) by electrocoagulation (EC) was investigated in a stirred tank reactor (STR), the effect of different influential parameters**,** namely, contact time, current density and pH was determined. Over 72 % of COD, 93 % of polyphenols and 95 % of color intensity were removed efficiently at pH of 5.2, current density of 58.33 mA/cm^2 and a residence time of 45 min. A kinetic study of these three parameters was carried out and both COD and dark color removal obey the first-order law model. On the other hand, the polyphenols reduction, fits the pseudo second-order model with current- dependent parameters. A variable order kinetic (VOK) model derived from the Langmuir-Freundlish equation was proposed to determine the kinetics of pollutant removal reactions with EC. Results showed that the model equations strongly fit the experimental concentrations of the three pollutants.

Keywords: Olive mill wastewater; electrocoagulation; COD; polyphenols; kinetic study; variable order kinetic

* Correspondence to: Reda Elkacmi. E-mail: redakcm@gmail.com

INTRODUCTION

Extraction of olive oil using three-phase decanter methods and traditional press generates a significant amount of a highly contaminated wastewater that requires treatment before discharge into the environment. The annual production of olive mill wastewater (OMW) in the Mediterranean region exceeds 30 million m^3 per year (Yahiaoui *et al.*, 2011; Casa *et al.*, 2003). In addition to their acidic pH (about 5), this effluent is characterized by very high chemical oxygen demand (COD) values (80−200 g/l), biological oxygen demand BOD values (12−60 g/l), polyphenolic compounds (up to 80 g/l), and total solids content (40−150 g/l) (Panizza & Cerisola, 2006, Ün *et al.*, 2006).

As environmental regulations became more strict and stringent, different technologies have been proposed to minimize the environmental impact of OMW, such as aerobic and anaerobic biological treatment (Benitez *et al.*, 1997; Bertin *et al.*, 2004), composting, fertilization, and animal feeding (Zenjari *et al.*, 2006; Cereti *et al.*, 2004; Hamdi, 1993), dilution, evaporation, sedimentation, filtration and centrifugation (Paraskeva *et al.*, 2007; Achak *et al*., 2009), physico-chemical processes such as coagulation-floculation (Jaouani *et al.*, 2005), thermochemical treatment (Guida *et al*., 2016), as well as other techniques for the production and recovery of natural products from this effluents (Elkacmi *et al*., 2016; Kaleh & Geißen, 2016; De Marco *et al*., 2007).

Recently, the electrocoagulation (EC) process was found to be an effective technique for the treatment of wastewaters, mainly owing to its simplicity, low energy consumption, effectiveness, low sludge formation and low dissolved solids. This technique have been used for the treatment of water containing dyes and textile wastes (Bennajah *et al.*, 2009; Alinsafi *et al.*, 2005), restaurant wastes (Chen *et al.*, 2000), oil refinery (Un *et al.*, 2009), suspended particles (Matteson *et al.*, 1995), leachate (Meunier *et al.*, 2006), heavy metal (Kabdaşli *et al.*, 2009), chemical and mechanical polishing (Belongia *et al.*, 1999), and mine wastes (Jenke & Diebold, 1984).

In the electrocoagulation process, the coagulant is generated in situ by dissolving electrically either aluminum or iron ion materials at the anode. Electrolytic gases (typically H_2) are released around the cathode. Several authors confirmed that aluminum is very effective for pollutants removal, especially organic (Can *et al.*, 2003; Bensadok *et al.*, 2008) and inorganic (Guzmán *et al.*, 2016; Heidmann & Calmano, 2008) matter from wastewater. The electrochemical reactions occurring at the electrodes are:

Anode (Aluminum oxidation):

$$Al(s) \longrightarrow Al^{3+} + 3e^-$$

Cathode (water reduction):

$$2H_2O + 2e^- \longrightarrow H_2(g) + 2OH^-$$

The sacrificial anodes deliver Al^{3+} which are hydrolyzed as a function of pH to produce aluminum hydroxide $Al(OH)_3$ and are then polymerized to $Al_n(OH)_{3n}$ which has strong affinity toward forming aggregates with pollutants. Evolution of hydrogen gas helps in mixing and flocculation. Once the floc is generated, the hydrogen gas bubbles carry the pollutant towards the liquid surface where it can be easily concentrated, collected, and removed (Holt *et al.*, 1999).

$$Al^{3+} + 3\,H_2O \longrightarrow Al(OH)_3 + 3H^+$$

$$n\,Al(OH)_3 \longrightarrow Al_n(OH)_{3n}$$

Several studies have proved that electrocoagulation are a very effective tool for the elimination of polyphenols, COD and color content of olive mill wastewater (Ün *et al*., 2006; Adhoum & Monser, 2004; Inan *et al*., 2004).

Abundant studies were performed on olive mill wastewater treatments using EC, for example Adhoum & Monser, 2004), who can remove more than 76 % COD, 91 % of polyphenols and 95 % of dark color. Nevertheless there remains a paucity of data concerning the mechanism of the pollutants removal from this type of effluent.

The purpose of the present work is to evaluate the removal of COD, polyphenols and dark color from OMW. Furthermore, the study of the operational parameters influence such as EC time, current density and pH, in order to determine for the first time, the kinetic of the removal of pollutants will be performed in order to estimate the time required for treatment. In addition, a modeling approach was conducted to simulate EC data for a better understanding of the mechanisms for OMW treatment.

MATERIAL AND METHODS

Characteristics of olive mill wastewater

Olive mill wastewater was obtained from an olive oil producing plant in Béni Mellal-Khénifra region, central of Morocco. OMW was collected in a closed plastic container and stored at ambient temperature. The main characteristics of OMW used in this work are presented in **Table 1**.

Table 1: Main characteristics of the raw OMW used in this study

Parameter	Value
pH	5.2
Conductivity (mS/cm)	5.1
Total polyphenols (g/l)	3.75
Total suspended solids (g/l)	0.84
COD (g/l)	27.6
DBO (g/l)	13.42
Absorbance (278 nm)	15.6
Absorbance (395 nm)	8.5

Electrochemical cell

The electrochemical treatment of OMW was studied in continuously stirred tank reactor (CSTR), consisted of two aluminum electrodes with rectangular geometry with the dimensions of 120 mm × 50 mm × 2 mm. The electrodes were disposed vertically at a distance of 1 cm from each other, and 2 cm from the bottom. The total effective surface area of plates immersed in OMW was 60 cm2 with a rotational stirring rate of about 400 roun the volume of the OMW treated was 3.5 dm^3.

The plates were connected to a direct current (DC) power supply providing voltage in the range of 0–30 V (0−6 A). The current intensity was measured by an amperemeter. Current density values (j) between 25 and 66.66 mA/cm^2 were investigated, which corresponded to an electric current (I = j.S) in the range of 1.5– 4 A.

Analytical methods

Before analyzing the evolution of COD, polyphenols and dark color intensity, the sample was filtrated using filtration papers (0.45 m, Millipore, USA).

The pH and conductivity were measured using a ProfilLine pH197i pHmeter (WTW, Germany) and CD-810 conductimeter (Radiometer Analytical, France).

The chemical oxygen demand (COD) and suspended solids (SS) were measured according to the standard methods for the examination of Water and Wastewater (APHA, 1998). Color intensity was determined via measuring the sample absorbance at 395 nm (9ol anak sta3melti spectrophotometer) (Sayadi *et al.*, 1996).

The initial concentration of polyphenols was determined using the Folin–Ciocalteu reagent according to the procedures developed in (Folin & Ciocalteau, 1927), Monitoring the total polyphenols, during treatment, was carried out by measuring the absorbance at 278 nm (Esfandyari *et al.*, 2014).

The removal rate (pourcentage) of COD, polyphenols and dark color from OMW by electrocoagulation was calculated as follow:

$$Y(\%) = \frac{COD_0 - COD}{COD_0} \times 100 \quad (1)$$

$$Y(\%) = \frac{A_0 - A}{A_0} \times 100 \quad (2)$$

$Y_{(PP)}$ and $Y_{(colo)}$ were calculated using the same equation, **Eq. (2)**, based on absorbance measurements at 278 nm and 395 nm respectively.

The specific electrical energy consumption in kWh/m^3 (E) was calculated using the following formula:

$$E(kWh/m^3) = \frac{U \times I \times t}{V} \quad (3)$$

where U: applied voltage (V); I: current intensity (A), t: retention time (h); V: volume of the treated olive mill wastewater (l)

The amount of electrodes dissolved per unit volume of treated olive mill wastewater, was calculated using Faraday's law:

$$C_{Al}(kgAl/m^3) = \frac{I \times t \times M}{Z \times F \times V} \times 10^{-3}$$

where I: current intensity (A), t: time of electrolysis (s), M: the molecular weight of aluminium (26.98 g/mol), z: the number of electron transferred (z = 3), F: Faraday's constant (96 487 C/mol), V: the volume of the treated olive mill wastewater in m^3.

RESULTS AND DISCUSSION

Effect of operating time on the removal of COD, polyphenols and dark color

Figure 1 illustrates the effect of the operating time on the evolution of the COD, polyphenols and dark color removal efficiency for the STR at (pH = 5.2, j = 50 mA/cm^2). It shows that the removal rate (percentage) of pollutants is high after 45 min of process, 69%, 86% and 89% of COD, polyphenols and dark color have been removed, respectively. The OMW samples during the treatment became visually very clear as shown in **Fig. 2**.

Effect of initial pH

Electrocoagulation process is reported to be strongly dependent on pH, **Fig. 3** illustrates the evolution of COD, PP and dark color removal efficiency at five various values of pH=2, 4, 5.2, 8 and 10, using hydrochloric acid and sodium hydroxide solutions. It is obvious that the removal efficiency presented a maximum corresponding to an initial pH about 5–6.

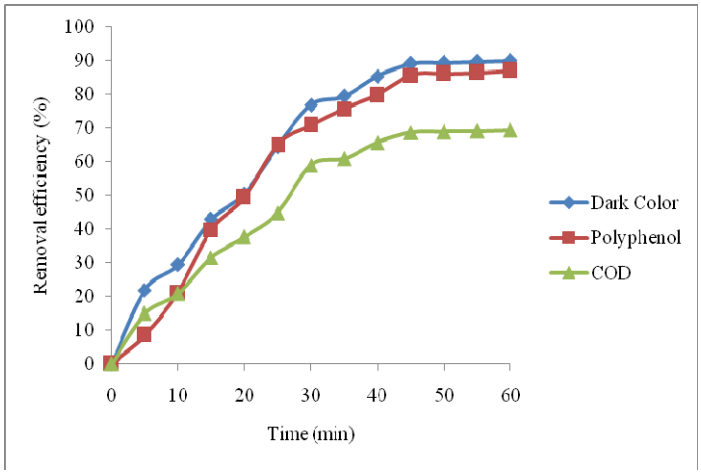

Fig. 1 Effect of operating time on the pollutants removal rate: COD; polyphenol and dark color (initial pH = 5.2, j = 50 mA/cm^2).

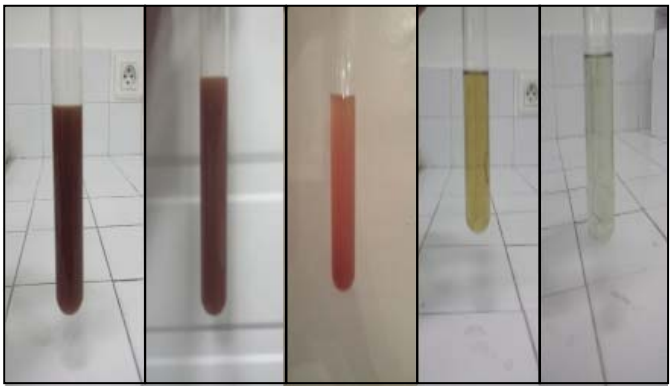

Fig. 2 Color change of OMW during treatment at (pH = 5.2, j =50 mA/cm^2).

Similar results have been previously reported by other authors (Holt *et al.*, 1999; Kul *et al.*, 2015; Hanafi *et al.*, 2010) who found that OMW can be treated directly without adjustment with chemical products (acid or base). Furthermore, during the process, the pH changed. Its evolution depended on the initial pH. In this work as in previous studies (Bennajah *et al.*, 2009; Kobya *et al.*, 2003), the pH tended towards about 7 which suggests that electrocoagulation exhibits a buffering effect, especially in an alkaline medium as shown in **Fig. 4**.

Effect of current density

Current density is an important parameter in the electrocoagulation process, which determines the coagulant production rate at the anode and the size of bubble production at the cathode.

The effect of current density variation on the COD, polyphenols and dark color removal efficiency is shown in **Fig. 5**.

When current density was varied from 25 to 66.66 mA/cm^2 the removal efficiency of COD, polyphenols and dark color were clearly rose from 59%, 65% and 76% to 75%, 93% and 97%, respectively after 45 min. At a density of 58.33 mA/cm^2 the removal

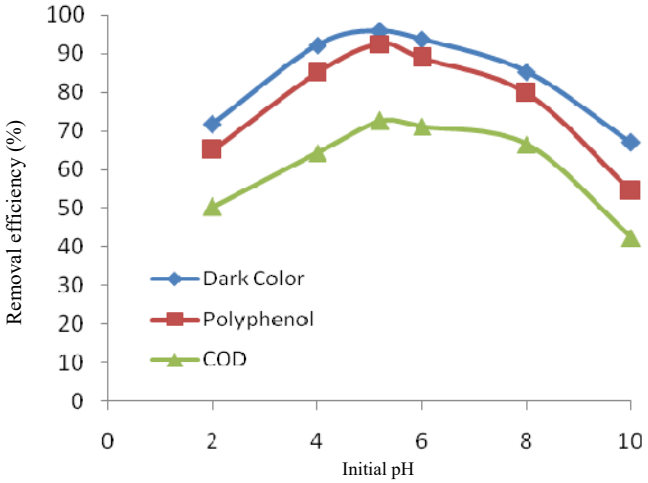

Fig. 3 Effect of initial pH on the pollutants removal rate: COD; polyphenol and dark color (j = 58.33 mA/cm^2).

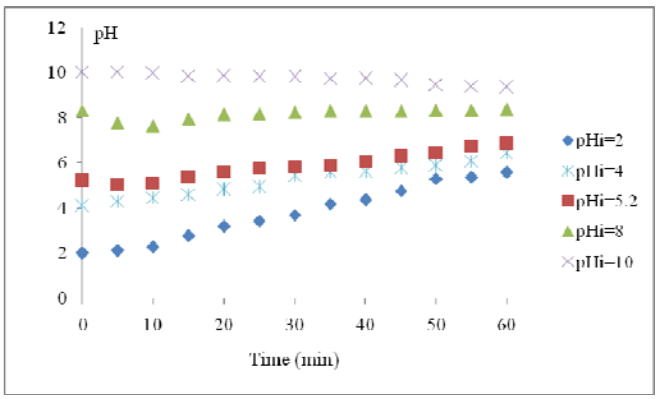

Fig. 4 Evolution of pH values during EC for different values of initial pH (j = 58.33 mA/cm^2).

(a)

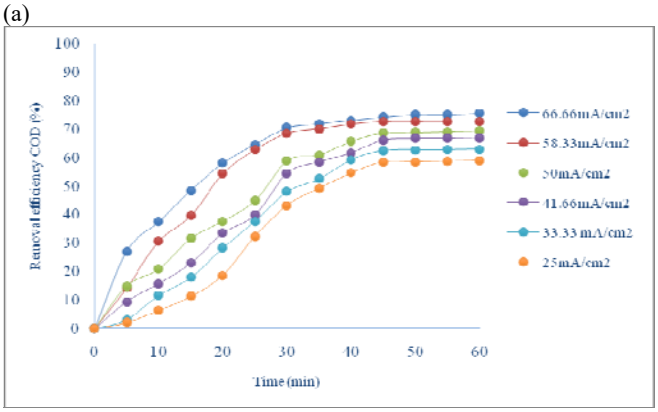

(b)

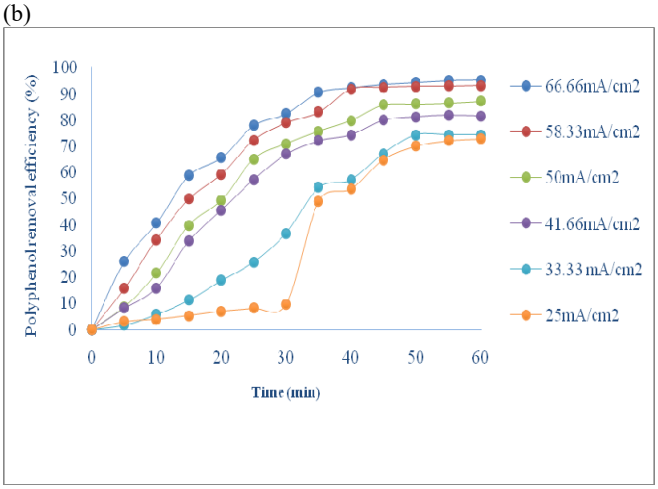

(c)

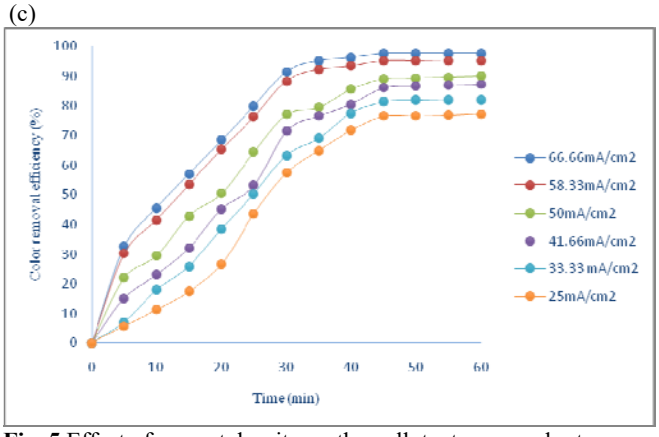

Fig. 5 Effect of current density on the pollutants removal rate: (a) COD; (b) polyphenol; (c) dark color (initial pH = 5.2).

efficiency of COD, polyphenols and dark color were 72%, 93% and 95%. Therefore the current density of 58.33 mA/cm^2 is chosen as an optimal current density for the treatment of OMW with respect to the maximum density 66.66 mA/cm^2, since it the quickest removal rate with the lowest cost (which will be examined later).

Kinetic study

In order to examine the removal of the pollutants, the mass conservation of pollutant is expressed as:

$$-\frac{dC}{dt} = r \quad (3)$$

where ($-r$) is the removal rate of pollutant in g/l, and t is the electrocoagulation time in min. For the first order model ($-r = k_1C$) and by integration, one may write:

$$\ln\left(\frac{C}{C_0}\right) = -k_1 t \quad (4)$$

The second-model order ($-r = k_2C$) and after integration is of the form:

$$\frac{1}{C} = \frac{1}{C_0} + k_2 t \quad (5)$$

The pseudo first-order can be expressed as:

$$\ln(C_e - C) = \ln C_e - k_3 t \quad (6)$$

The linear form of pseudo-second order model was expressed as:

$$\frac{t}{C} = \frac{1}{k_4 C_e^2} + \left(\frac{1}{C_e}\right) t \quad (7)$$

where k_1, k_2, k_3 and k_4 are the equilibrium rate constants in min^{-1}, and Ce is the amount of pollutant adsorbed at equilibrium in mol/l.

Determination of suspended solid concentration in (g/l) gives a linear relation ($R^2 = 0.988$) with color absorbance, as shown in **Fig. 6**.

It is clearly shown that suspended solid concentration increased proportionally to the color absorbance, this result can be used in the study of kinetics reduction of color intensity from olive mill wastewater.

The kinetic parameters of the four models with the R^2 values at different current densities are given in **Tables 2** and **3**. As can be seen, the color reduction can be described by first-order kinetics since the correlation coefficient (R^2) is mostly higher than 0.93%. For the polyphenols removal, except the lower density of 25 mA/cm^2, the R^2 values that correspond to the first-order model can also be a representative model to its removal rate.

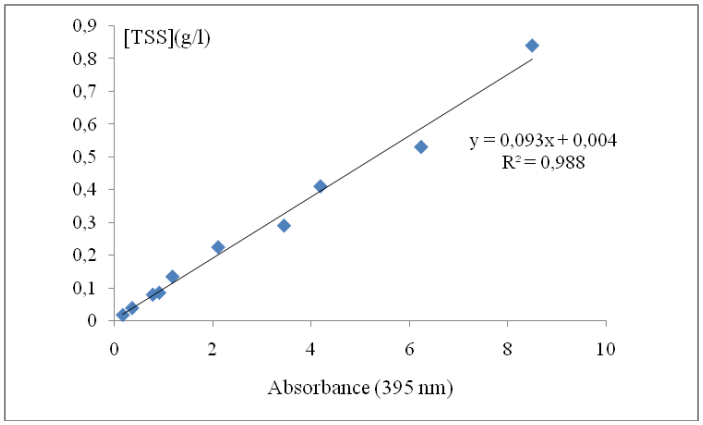

Fig. 6 Calibration curve of suspended solid (g/l)×absorbance at 395 nm.

Table 2. Comparison between the parameters of first- and second-order removal rates of COD polyphenols (PP) and dark color at different current densities with solution volume = 350 cm^3, initial pH= 5.2 and conductivity κ = 5.1 mS/ cm.

Parameters	CD (mA/cm^2)	First-order model		Second-order model	
		k_1(min^{-1})	R^2	k_2(min^{-1})	R^2
COD	25	0.0184	0.9417	0.0011	0.9433
	33.33	0.0198	0.9517	0.0013	0.9538
	41.66	0.0213	0.9510	0.0015	0.9566
	50	0.0218	0.9456	0.0016	0.9565
	58.33	0.0229	0.8627	0.0019	0.9073
	66.66	0.0227	0.8736	0.0020	0.9360
PP	25	0.0260	0.8695	0.0023	0.6830
	33.33	0.0273	0.9460	0.0037	0.8897
	41.66	0.0327	0.9649	0.0057	0.9631
	50	0.0389	0.9724	0.0084	0.9492
	58.33	0.0515	0.9597	0.0179	0.9004
	66.66	0.0558	0.9728	0.0245	0.9357
Color	25	0.0300	0.9492	0.0082	0.9336
	33.33	0.0342	0.9599	0.0111	0.9324
	41.66	0.0397	0.9636	0.0160	0.9286
	50	0.0435	0.9669	0.0211	0.9319
	58.33	0.0581	0.9389	0.0493	0.9142
	66.66	0.0728	0.9465	0.1033	0.8885

Table 3. Comparison between the parameters of pseudo first and pseudo second-order removal rates of COD, polyphenols (PP) and dark color at different current densities with solution volume = 350 cm^3, initial pH= 5.2 and conductivity κ = 5.1 mS/ cm

Parameters	CD (mA/cm^2)	Pseudo First-order model			Pseudo Second-order model		
		k_3 (min^{-1})	Ce (g/l)	R^2	k_4 (min^{-1})	Ce (g/l)	R^2
COD	25	0.0265	11.43	0.8572	0.0153	10.47	0.9713
	33.33	0.0293	10.35	0.8707	0.0165	9.43	0.9697
	41.66	0.0301	9.31	0.9182	0.0178	8.41	0.9676
	50	0.0340	8.61	0.9110	0.0195	7.80	0.9692
	58.33	0.0556	7.55	0.9498	0.0269	6.88	0.9844
	66.66	0.0533	7.11	0.9732	0.0284	6.32	0.9837
PP	25	0.0222	1.31	0.6027	0.0243	0.99	0.8829
	33.33	0.0291	1.22	0.8275	0.0275	0.90	0.8950
	41.66	0.0621	0.75	0.9584	0.0430	0.63	0.9357
	50	0.0861	0.53	0.9716	0.0535	0.44	0.9107
	58.33	0.4377	0.27	0.8046	0.0947	0.23	0.8847
	66.66	7.4686	0.24	0.9170	0.1230	0.17	0.8773
Color	25	0.0940	0.19	0.8640	0.0645	0.18	0.9360
	33.33	0.1494	0.15	0.8763	0.0775	0.13	0.9236
	41.66	0.3993	0.11	0.9225	0.0978	0.09	0.9052
	50	0.8696	0.09	0.9302	0.1229	0.07	0.9012
	58.33	0.1139	0.04	0.9331	0.2601	0.03	0.9028
	66.66	0.0670	0.02	0.9315	0.4763	0.02	0.8669

As can be observed in the **Table 2**, the correlation coefficient (R^2) of the COD removal for pseudo-second-order reaction are too close to unity ($R^2 \geqslant 0.9676$). Comparing the rate constants, it was found that increasing the current resulted in a significant increase of the rate constants. k_1= 0.0300 to 0.0728 min^{-1}, k_1= 0.0260 to 0.0558 min^{-1} and k_4=0.0153 to 0.0284 min^{-1} for dark color, polyphenols and COD removal respectively.

Adsorption equilibrium isotherms theory

In order to describe the adsorption capacity of a specific adsorbent, related to its active sites, it is necessary to relay on the adsorption isotherms. The adsorption equilibrium isotherms represent the adsorption equilibrium (adsorbed quantity) at different concentrations of the adsorbate, in an isotherm environment. On an experimental level, the adsorption equilibrium isotherms are performed by measuring the quantity adsorbed after reaching equilibrium for different concentration of adsorbent. The experiment should be performed at a fixed temperature. The adsorption equilibrium isotherm diagram isn't significant itself. It should there for be related to one of the 20 models developed, that allow a better apprehension of the adsorption isotherm data. The Langmuir model and Freundlich model, were found to fit most of adsorption isotherms data, and are by far the most widely used.

Langmuir model

Langumir model characterizes the adsorption as a monolayer adsorption, meaning that an active site only receives a single particle of adsorbate, after the layer (only layer here) is saturated; the adsorption reaches equilibrium as there are, in theory, no more active sites to host the adsorbate particles. The langumir adsorption isotherm is mathematically characterized by the **Eq. (8):**

$$q_e = \frac{q_{\max} k_L C_e}{1 + k_L C_e} \qquad (8)$$

where qe is the amount adsorbed at equilibrium (gram of adsorbate per gram of adsorbent), qmax is the maximum adsorption capacity (gram of adsorbate per gram of adsorbent), Ce is the equilibrium concentration of the adsorbate (g/l), and k_L is Langumir coefficient. The linearization of the **Eq. (8)** allows the numeric identification of the constants qmax and k_L.

Freundlich model

Freundlich model on the other hand, describes the multilayer adsorption. It is applicable mostly when the adsorbent has a great specific area. The multilayer adsorption means that the active sites of the adsorbent may receive more than a particle of the adsorbate. When the first layer is saturated, the adsorption continues on the second layer, formed by the juxtaposition of adsobate particles already adsorbed. The number of layers is limited though, depending on the adsorbent. The Freundlich model is mathematically modeled by the **Eq. (9)** where qe is the amount adsorbed at equilibrium (gram of adsorbate per gram of adsorbent), C_e is the equilibrium concentration of the adsorbate (g/l). k_F and

p are Freundlich constants to determine through the **Eq. (9)** linearization.

$$q_e = k_F C_e^{\frac{1}{p}} \qquad (9)$$

Langmuir–Freundlich combined model

Eventhough Langumir and Freundlich are the most used models to characterize the behavior of a adsorbate/adsorbent couple, the gap between theoretical results and experimental data may sometimes appear flagrant (Bennajah *et al.*, 2010). Thus limiting the applicability of theoretical results to an industrial plan. The combined Langumir –Freundlich was first proposed by (Bennajah *et al*., 2010) to a better modeling of a very similar adsorption case. Therefor, a modified combined model was applied to fit the equilibrium data, its validity will be confirmed further in this study. The langumir-Freundlich isotherm is mathematically modeled by the **Eq. (10)**.

$$q_e = \frac{q_{\max} k_{LF} C_e^n}{1 + k_{LF} C_e^n} \qquad (10)$$

where qe is the amount adsorbed at equilibrium (gram of removed pollutant per gram of $Al(OH)_3$), q_{max} is the maximum adsorption capacity, and k_{LF} are the equilibrium constants or the affinity parameters of binding sites (g/l), n is the constant which shows greatness of relationship between adsorbate and adsorbent (index of heterogeneity) and Ce is the equilibrium concentration of the adsorbate (g/l).

The experimental data of OMW treatment by electrocoagulation were obtained by changing current densities from 25 to 66.66 mA/cm^2, keeping all other experimental conditions constant (pHi = 5.2, V= 3.5 cm^3, t = 45 min).

The adsorption capacity, q_e (g/g), was calculated as follows:

$$q_e = \frac{(C_0 - C_e)V}{m} \qquad (11)$$

where C_0 and C_e are the initial concentration and concentration at equilibrium (g/l), respectively, V volume of solution (l) and m is the mass of adsorbent $Al(OH)_3$ (g) released from the anode obtained by the electrode mass difference before and after electrocoagulation process..

The Langmuir and Frendlish parameters were determined by plotting Ce/qe versus Ce and ln qe against ln Ce, respectively based on the linear forms of models. For the model of Langmuir-Freundlich (LF), qe was directly plotted against Ce, and the three parameters (q_{max}, k_{LF} and n) were determined by nonlinear regression method using the solver add-in function of the Microsoft Excel by minimum chi-square estimation:

Table 4: Langmuir, Freundlich and Langmuir-Freundlich isotherm parameters for COD and polyphenols adsorption

COD			
	Langmuir	Frendlish	Langmuir-Frendlish
q_{max} (g/g)	9.708	-	23.95
k_L (g/l)	0.075	-	-
k_F (g/l)	-	0.019	-
k_{LF} (g/l)	-	-	0.249
n	-	-	0.997
p	-	0.312	-
R^2	0.790	0.943	0.991
Polyphenols			
	Langmuir	Frendlish	Langmuir-Frendlish
q_{max} (g/g)	3.507	-	7.355
k_L(g/l)	0.717	-	-
k_F (g/l)	-	1.469	-
k_{LF} (g/l)	-	-	0.264
n	-	-	0.823
p	-	1.437	-
R^2	0.481	0.844	0.992
Color			
	Langmuir	Frendlish	Langmuir-Frendlish
q_{max} (g/g)	0.534	-	55.314
k_L(g/l)	12.07	-	-
k_F (g/l)	-	1.304	-
k_{LF} (g/l)	-	-	0.029
n	-	-	0.727
p	-	1.533	-
R^2	0.927	0.903	0.993

$$\chi^2 = \sum \frac{(q_{\text{mod}} - q_{\exp})^2}{q_{\exp}} \qquad (12)$$

The coefficient of the three models with the regression coefficients R^2 are reported in **Table 4**. As can be observed, the Langmuir–Freundlich model can be used to ensure a better representation of the experimental data of adsorption isotherms.

Variable Order Kinetic approach

In fact, the kinetic model can't faithfully describe the adsorption phenomenon in this case. Hu *et al.* (2007) stated that a flagrant gap was noticed between the calculated resident time and the effective resident time measured in industrial plants. It is in fact inaccurate to base the resident time calculations only on the kinetic model, since it neglects the capacity of the adsorbent as an influencing factor.

VOK model (Variable Order Kinetic) was developed in order to best represent experimental results. The aim of the VOK is to describe as accurately as possible the

adsorption kinetics for a comprehensive estimation of the time required for treatment due to the change in mass of adsorbent. By presenting a comprehensive mathematical model, where all factors are taken into consideration.

This model was proposed by (Hu *et al.*, 2007) based on Langmuir isotherm in order to estimate the time required to defluoridation by EC in a 1L stirred cell. (Bennajah *et al*., 2010) developed a similar approach in two batch reactors (20 L): a stirred tank reactor (STR) and an external-loop airlift reactor (ALR) to describe the kinetics of fluoride removal based on the Langmuir-Freundlish equation.

The VOK model was conducted for the first time to describe and study the EC mechanisms effect of detoxification of OMW in (STR) using aluminum electrodes.

The concept of the model based on the combination of the three following laws:

- Faraday law, **Eq. (4)**.
- Constant current density, detoxification is proportional to the production of aluminum in solution, with a close current efficiency (ϕ_c).
- The adsorption equilibrium model.

As shown in the kinetic study part, the floc formation and the precipitation of $Al(OH)_3$ followed first order kinetic for the color and polyphenols reduction and pseudo-second-order for COD removal.

As demonstrated previously, the treatment rate in the VOK approach is related to the kinetics of aluminium release, expressed as the total aluminium concentration in solution $[Al]_{Tot}$. Considering that the adsorption is instantaneous and that the adsorbent formed is permanently in the adsorption equilibrium with the pollutants in solution, the detoxification rate can be expressed as follows:

$$-\frac{dC}{dt} = \phi_{Al} q_e \frac{d[Al]_{Tot}}{dt} \qquad (13)$$

where ϕ_{Al} is the efficiency of the formation of flocs and $[Al]_{tot}$ is the total aluminium dosage liberated from the anode which can be determined from Faraday's law:

$$-\frac{d[Al]_{Tot}}{dt} = \phi_C q_e \frac{I}{ZFV} \qquad (14)$$

where ϕ_c is the current efficiency (faradic yield), I is the applied current (A), Z is the valence of the Al (Z = 3), F is Faraday's constant and V is the volume of the reactor (m^3).

The result of the combination of both **Eqs (13)** and **(14)** with **Eq. (10)** was illustrated as:

$$-\frac{dC}{dt} = \phi_{Al}\phi_C \frac{q_{\max} k_{LF} C_e^n}{1 + k_{LF} C_e^n} \frac{I}{ZFV} \qquad (15)$$

The first-order rate constant (k_1) can be expressed as **Eq. (16)**:

$$k_1 = \phi_{Al}\phi_C \frac{q_{\max} k_{LF} C_e^{n-1}}{1 + k_{LF} C_e^{n-1}} \frac{I}{ZFV} \qquad (16)$$

Using **Eq. (15)**, the pseudo-second-order rate constant (k_4) can be expressed as follows:

$$k_4 = \phi_{Al}\phi_C \frac{q_{\max} k_{LF} C_e^n}{\left(1 + k_{LF} C_e^{n-1}\right)\left(C - C_e\right)^2} \frac{I}{ZFV} \qquad (17)$$

By integrating **Eq. (15)**, the retention time required (t_N) to eliminate an acceptable concentration of pollutants (C_e) can be expressed as:

$$t_N = \frac{ZFV}{\phi_{Al}\phi_C I q_{\max}} \left[\left(C_0 - C\right) + \frac{1}{k_{LF}(1-n)} \left(C_0^{1-n} - C^{1-n}\right) \right] \qquad (18)$$

The (VOK) model derived from the Langmuir-freundlish equation will be applied to the experimental data obtained in Section 3.3, the effect of current density was studied at optimal conditions (pHi = 5.2 and t = 45 min).

Figure 7 shows the variations of pollutants concentration during EC and (VOK) model versus time at I= 1.5, 2, 2.5, 3, 3.5 and 4 A corresponding to a current densities of CD = 25, 33.33, 41.66, 50, 58.33 and 66.66 mA/cm^2, respectively.

As it can be seen, the VOK model strongly fits the experimental data. Thus demonstrating the validity of VOK in modelling the detoxification of OMW phenomenon with various current densities. The parameters q_{max} and k_{LF} for the three pollutants were not varied with current densities and n>1 indicating that the adsorption on the floc takes place on the external surface and intercalation into the interlayer space at the same time (positive cooperativity) (**Table 5**).

The effect of CD variation on treatment of OMW was investigated, at I< 3A corresponding to a current density of 58.33 mA/cm^2, the kinetics of pollutants removal, especially polyphenols was not exactly proportional to current in the experiments, while for higher currents, a good fitting of the experimental data was obtained using Langmuir–Freundlich isotherm. The coefficient n is nearly constant and the corresponding χ 2 values at all current densities have an average minimum value of around χ 2 = 0.56, 1.47, 0.75 for COD, PP and color, respectively.

(a)

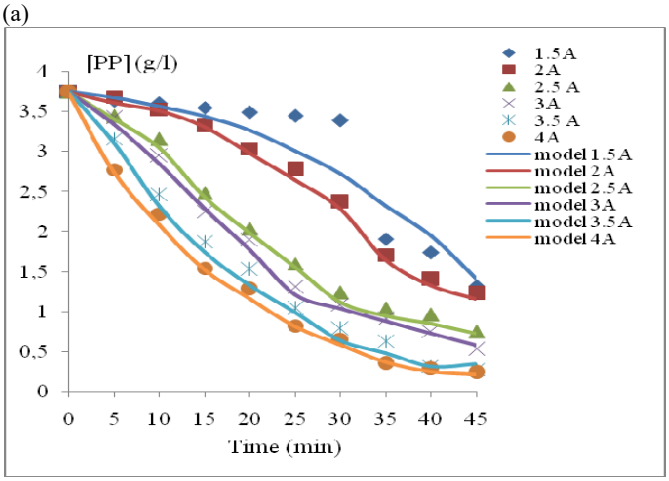

(b)

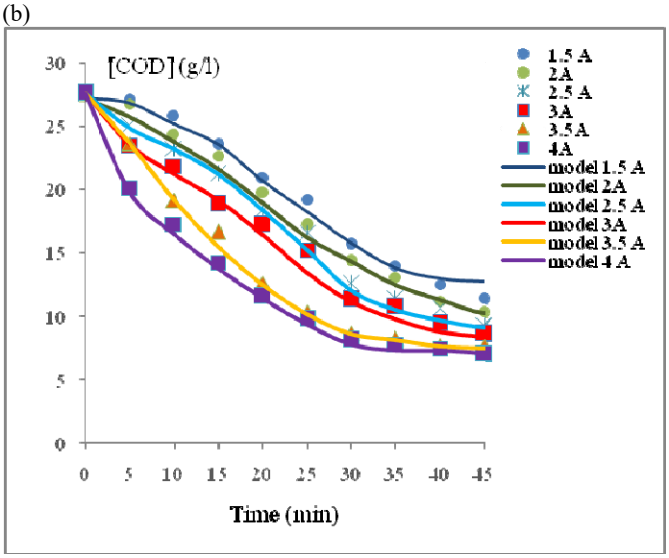

(c)

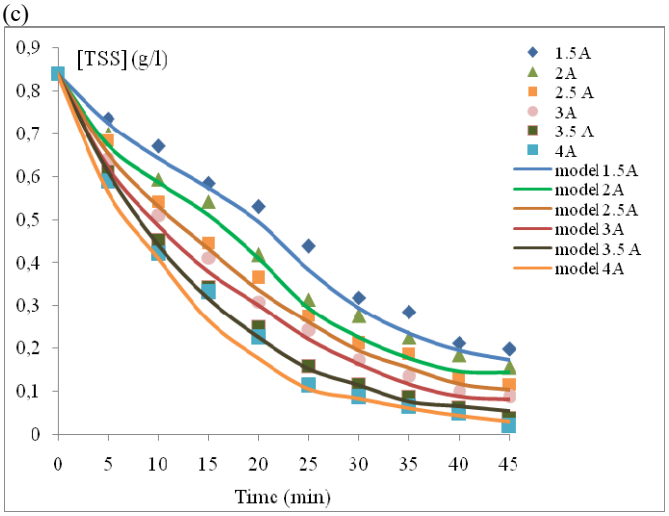

Fig. 7. Variations of pollutants concentration during EC (pHi = 5.2, t = 45min) at different applied current densities and comparison with the predictions of the VOK model: (a) Polyphenols (b) COD (c) Total suspended solids.

Energy and electrodes consumptions

Electrical energy consumption is one of the most important economical parameters in the electrocoagulation process. Therefore, in the same operation conditions (pHi = 5.2, V = 3.5 cm^3), after 45min and 60 min of electrocoagulation), the amount of dissolved electrodes C_{Al} ($kgAl/m^3$), the electrical energy consumption E (kWh/m^3) and the corresponding removal efficiencies for the three pollutants at different current densities is also represented in **Table 6** and **Fig. 8**.

As seen in **Table 6**, when the current density was increased from 25 to 66.66 mA/cm^2, the theoretical concentration of aluminum was increased from 0.107 to 0.383 $kgAl/m^3$ and the power requirement was increased from 1.01 to 31.35 kWh/m^3 after EC treatment time varied between 45 and 60 min as demonstrated in many electrolytic studies (Panizza & Cerisola, 2006; Chen *et al.*, 2000; Martinez-Huitle & Brillas, 2009).

After 45 min EC treatment, the removal efficiencies ranged between 58.57–74.24%, 64.84-93.26% and 76.46-97.64% for COD, polyphenols and dark color, respectively. These results can be explained by the fact that, the extent of anodic dissolution of aluminum increases, resulting in a greater amount of aluminum hydroxides $Al(OH)_{3(s)}$ necessary to form coagulants (according to Faraday's Law) (Lemlikchi *et al.*, 2012; Bazrafshan *et al.*, 2016).

As mentioned above, when the current density was raised to 58.33 mA/cm^2 the removal efficiency of COD, polyphenols and dark color rose to 72.63%, 92.53% and 95.20%, respectively after 45 min of EC treatment and the corresponding consumptions of electrical energy with the amount of dissolved electrodes were 23.51 kWh/m^3 and 0.287 $kgAl/m^3$, respectively. Furthermore, it is seen that after one hour of treatment the removal efficiency of pollutants remained approximately constant for current density greater than 58.33 mA/cm^2, 75.55%, 93.41% and 97.66% of DCO, PP and dark color have been removed, accompanied by a consumption of 31.35 kWh/m^3 and 0.383 $kgAl/m^3$, for electrical energy and aluminium electrode, respectively, which proves that the best EC in terms of lowest energy consumption and cost of aluminum dosed was obtained at this optimum value.

In addition, **Fig. 8** illustrates the effect of current density on electrodes consumption (anode + cathode) compared with the theoretical mass. As per **Fig. 8**, for the optimim value of CD = 58.33 mA/cm^2, the experimental amount of dissolved Aluminium from the loss of anode mass had a value of 0.314 kg Al/m^3 exceeding the theoretical value (0.287 kg Al/m^3). Beyond this point, a very important difference will be observed, this mass overconsumption of aluminum electrodes explained by the fact that, at higher currents, the supply of aluminum ions is generated rapidly, due to the chemical hydrolysis of the cathode, and the "corrosion pitting" phenomenon which causes holes on the electrode surface (Holt *et al.*, 2002; Essadki *et al.*, 2008).

Table 5: Values of n using the VOK model coupled with Langmuir–Freundlich isotherm: influence of current density (pHi = 5.2, t = 45min)

				Removal efficiency (%)		
CD (mA/cm^2)	t (min)	C_{Al} (kgAl/m^3)	E (kWh/m^3)	COD	PP	Color
25	45	0.107	1.01	58.57	64.84	76.46
25	60	0.143	1.35	59.13	72.92	77.15
33.33	45	0.143	3.11	62.46	67.22	81.32
33.33	60	0.191	4.15	63.01	74.35	82.00
41.66	45	0.179	5.62	66.26	79.97	86.06
41.66	60	0.239	7.49	67.08	81.49	87.08
50	45	0.215	8.98	68.78	85.83	89.20
50	60	0.287	11.97	69.49	87.15	90.09
58.33	45	0.251	16.21	72.63	92.53	95.20
58.33	60	0.335	21.61	72.82	93.19	95.18
66.66	45	0.287	23.51	74.24	93.26	97.64
66.66	60	0.383	31.35	75.55	93.41	97.66

Table 6: Electrical energy and removal efficiencies at different current densities and EC time with solution volume = 350 cm^3, pHi = 5.2.

	COD		PP		Color	
CD (mA/cm^2)	n	χ^2	n	χ^2	n	χ^2
25	1.315	0.75	1.276	1.96	1.141	0.96
33.33	1.324	0.64	1.274	1.25	1.141	0.74
41.66	1.331	0.59	1.281	1.86	1.153	0.73
50	1.354	0.45	1.291	1.34	1.165	0.88
58.33	1.321	0.58	1.281	1.29	1.155	0.52
66.66	1.364	0.37	1.296	1.15	1.086	0.71

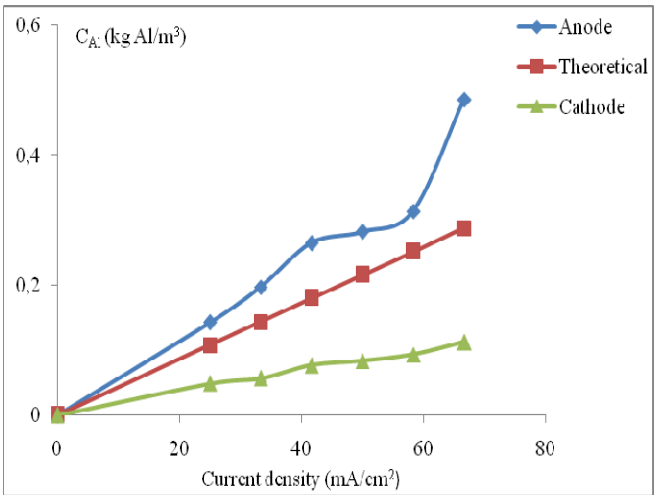

Fig. 8 Effect of current density on electrodes consumption. (pHi = 5.2, t = 45 min).

CONCLUSION

In this paper, a variable order kinetic model (VOK) was applied to better understand the kinetics of the detoxification of olive mill wastewater with EC using aluminum electrodes. A variable (VOK) model derived from the Langmuir-Freundlich equation has been successfully applied for the first time to describe the removal rates of COD, polyphenols and dark color from this types of OMW. Since the agreement between the predictive equations and experimental kinetic data were satifcatory, and the values of the critical parameters q_{max}, k_{LF} and n stay constant as the current density increases.

The effects of the different operational parameters were investigated. The results showed that electrocoagulation can remove 72.63% of COD, 92.53% of polyphenols and 95.20% of dark color, just after 45 min of treatment without any pH adjustment. In addition, it was demonstrated that the reduction rate of COD follows pseudo-second-order, and first-order model is more appropriate to represent reduction rate of polyphenols and dark color.

As a conclusion, the variable order kinetic (VOK) approach coupled with a Langmuir–Freundlich adsorption isotherm can be used to simulate electrocoagulation data, in order to predict the experimental conditions, for performing an effective OMW treatment.

REFERENCES

Achak, M., Mandi, L., Ouazzani, N. (2009) Removal of organic pollutants and nutrients from olive mill wastewater by a sand filter. *J. Environ. Manage.* **90**(9) 2849–2930. Doi: 10.1016/j.jenvman.2009.03.012

Adhoum, N. & Monser, L. (2004) Decolourization and removal of phenolic compounds from olive mill wastewater by electrocoagulation. *Chem. Eng. Process. Process Intensif*, **43**(10), 1281–1287. Doi: 10.1016/j.cep.2003.12.001

Alinsafi, A., Khemis, M., Pons, M.N., Leclerc, J.P., Yaacoubi, A., Benhammou, A., Nejmeddine, A. (2005) Electro-coagulation of reactive textile dyes and textile wastewater. *Chem. Eng. Process. Process Intensif*, **44**(4), 461–470. Doi: 10.1016/j.cep.2004.06.010

APHA (1998) Standard Methods for the Examination of Water and Wastewater, 18th ed. American Public Health Association, Washington, DC, USA.

Bazrafshan, E., Alipour, M.R., Mahvi, A.H. (2016) Textile wastewater treatment by application of combined chemical coagulation, electrocoagulation, and adsorption processes. *Desalin. Water Treat*, **57**(20), 9203–9215. Doi: 10.1080/19443994.2015.1027960

Belongia, B.M., Haworth, P.D., Baygents, J.C., Raghavan, S. (1999) Treatment of alumina and silica chemical mechanical polishing waste by electrodecantation and electrocoagulation. *J. Electrochem. Soc*, **146**(11), 4124–4130.

Benitez, J., Beltran-Heredia, J., Torregrosa, J., Acero, J. L., Cercas, V. (1997) Aerobic degradation of olive mill wastewaters. *Appl. Microbiol. Biotechnol*, **47**(2), 185–188. Doi: 10.1007/s002530050910

Bennajah, M., Gourich, B., Essadki, A. H., Vial, C., Delmas, H. (2009) Defluoridation of Morocco drinking water by electrocoagulation/electroflottation in an electrochemical external-loop airlift reactor. *Chem. Eng. J.* **148**(1), 122–131. Doi: 10.1016/j.cej.2008.08.014

Bennajah, M., Maalmi, M., Darmane, Y., Touhami, M.E. (2010) Defluoridation of drinking water by electrocoagulation/electroflotation: kinetic study. *J. Urban Environ. Enging.* **4**(1), 37–45. Doi: 10.4090/juee.2013.v4n1.

Bensadok, K. S., Benammar, S., Lapicque, F., Nezzal, G. (2008) Electrocoagulation of cutting oil emulsions using aluminium plate electrodes. *J. Hazard. Mater.* **152**(1), 423–430. Doi: 10.1016/j.jhazmat.2007.06.121

Bertin, L., Berselli, S., Fava, F., Petrangeli-Papini, M., Marchetti, L. (2004) Anaerobic digestion of olive mill wastewaters in biofilm reactors packed with granular activated carbon and «Manville » silica beads. *Water Res*, **38**(14-15), 3167–3178. Doi: 10.1016/j.watres.2004.05.004

Can, O.T., Bayramoglu, M., Kobya, M. (2003) Decolorization of reactive dye solutions by electrocoagulation using aluminum electrodes. Ind. *Eng. Chem. Res*, **42**(14), 3391–3396. Doi: 10.1021/ie020951g

Casa, R., D'Annibale, A., Pieruccetti, F., Stazi, S.R., Gionanorozzi Sermani, G., Lo Cascio, B. (2003) Reduction of the phenolic components in olive-mill wastewaters by an enzymatic treatment and its impact on durum wheat (Triticum durum Desf) germinability. *Chemosphere*, **50**(8), 959–966. Doi: 10.1016/S0045-6535(02)00707-5

Cereti, C.F., Rossini, F., Federici, F., Quaratino, D., Vassilev N., Fenice M. (2004) Reuse of microbially treated olive mill wastewater as fertiliser for wheat (*Triticum durum Desf.*). *Bioresour. Technol*, **91**(3), 135–140. Doi: 10.1016/S0960-8524(03)00181-0

Chen, X., Chen, G., Yue, P.L. (2000) Separation of pollutants from restaurant wastewater by electrocoagulation. *Sep. Purif. Techno*, **19**(1), 65–76. Doi: 10.1016/S1383-5866(99)00072-6

De Marco, E., Savarese, M., Paduano, A., Sacchi, R. (2007) Characterization and fractionation of phenolic compounds extracted from olive oil mill wastewaters. *Food Chem*, **104**(2), 858–867. Doi: 10.1016/j.foodchem.2006.10.005

Elkacmi, R., Kamil, N., Bennajah, M., Kitane, S. (2016) Extraction of Oleic Acid from Moroccan Olive Mill Wastewater. *Biomed Res. Int*. ID 1397852, 1–9. Doi: 10.1155/2016/1397852

Esfandyari, Y., Mahdavi, Y., Seyedsalehi, M., Hoseini, M., Safari, G.H., Ghozikali, M.G., Kamani, H., Jaafari, J. (2014) Degradation and Biodegradability Improvement of the Olive Mill Wastewater by Peroxi-Electrocoagulation/Electrooxidation-Electroflotation Process with Bipolar Aluminum Electrodes. *Environ. Sci. Pollut. Res.* **22**(8), 6288–6297. Doi: 10.1007/s11356-014-3832-5

Essadki, A.H., Bennajah, M., Gourich, B., Vial, Ch., Azzi, M., Delmas, H. (2008) Electrocoagulation/electroflotation in an external-loop airlift reactor—application to the decolorization of textile dye wastewater: a case study. *Chem. Eng. Process*. **47**(8), 1211–1223. Doi: 10.1016/j.cep.2007.03.013

Folin, O. & Ciocalteau. U. (1927) On tyrosine and tryptofan determinations protein. *J. Biol. Chem.* **73**, 627–650.

Guida, M.Y., Bouaik, H., Tabal, A., Hannioui, A., Solhy, A., Barakat, A., Aboulkas, A. (2016) Thermochemical treatment of olive mill solid waste and olive mill wastewater. *J. Therm. Anal. Calorim*, **123**(2), 1657–1666. Doi: 10.1007/s10973-015-5061-7

Guzmán, A., Nava, J.L., Coreño, O., Rodríguez, I., Gutiérrez, S. (2016) Arsenic and fluoride removal from groundwater by electrocoagulation using a continuous filter-press reactor. *Chemosphere*, **144**, 2113–2120. Doi: 10.1016/j.chemosphere.2015.10.108

Hamdi, M. (1993) Future prospects and constraints of olive mill wastewaters use and treatment: a review. *Bioprocess. Enging*. **8**(5-6), 209–214. Doi: 10.1007/BF00369831

Hanafi, F., Assobhei, O., Mountadar, M. (2010) Detoxification and discoloration of Moroccan olive mill wastewater by electrocoagulation. *J. Hazard. Mater.* **174**(1), 807-812. Doi: 10.1016/j.jhazmat.2009.09.124

Heidmann, I., Calmano, W., 2008. Removal of Zn (II), Cu (II), Ni (II), Ag (I) and Cr (VI) present in aqueous solutions by aluminium electrocoagulation. *J. Hazard. Mater.* **152**(3), 934–941. Doi: 10.1016/j.jhazmat.2007.07.068

Holt, P.H., Barton, G.W., Mitchell, A.A., 1999. Electrocoagulation as a wastewater treatment. *Proc. The Third Annual Australian Environmental Engineering Research Event*. Castlemaine, Victoria, 23–26 November.

Holt, P.H., Barton, G.W., Wark, M., Mitchell, A.A. (2002) A quantitative comparison between chemical dosing and electrocoagulation. *Colloids Surf. A: Physicochem. Eng. Aspects* **211**(2-3), 233–248. Doi: 10.1016/S0927-7757(02)00285-6

Hu, C.Y., Lo, S.L., Kuan, W.H. (2007) Simulation the kinetics of fluoride removal by electrocoagulation (EC) process using aluminium electrodes, *J. Hazard. Mater*. 145 180–185. Doi: 10.1016/j.jhazmat.2006.11.010

Inan, H., Dimoglo, A., Şimşek, H., Karpuzcu, M. (2004) Olive oil mill wastewater treatment by means of electro-coagulation. *Sep. Purif. Technol,* **36**(1), 23–31. Doi: 10.1016/S1383-5866(03)00148-5

Jaouani, A., Vanthournhout, M., Penninckx, M. J. (2005) Olive oil mill wastewater purification by combination of coagulation-flocculation and biological treatments. *Environ. Technol*, **26**(6), 633–642. Doi: 10.1080/09593330.2001.9619503

Jenke, D.R. & Diebold, F.E. (1984) Electroprecipitation treatment of acid mine wastewater. *Water Res*, **18**(7), 855–859. Doi: 10.1016/0043-1354(84)90269-0

Kabdaşli, I., Arslan, T., Ölmez-Hanci, T., Arslan-Alaton, I., Tünay, O. (2009) Complexing agent and heavy metal removals from metal plating effluent by electrocoagulation with stainless steel electrodes. *J. Hazard. Mater.* **165**(1), 838–845. Doi: 10.1016/j.jhazmat.2008.10.065

Kaleh, Z. & Geißen, S.U. (2016) Selective isolation of valuable biophenols from olive mill wastewater. *J. Environ. Chem. Eng*, **4**(1), 373–384. Doi: 10.1016/j.jece.2015.11.010

Kobya, M., Can, O.T., Bayramoglu, M. (2003) Treatment of textile wastewaters by electrocoagulation using iron and aluminum electrodes. *J. Hazard. Mater.* **100**(1), 163–178. Doi: 10.1016/S0304-3894(03)00102-X

Kul, S., Boncukcuoğlu, R., Yilmaz, A. E., Fil, B. A. (2015) Treatment of olive mill wastewater with electro-oxidation method. *J. Electrochem. Soc*, **162**(8), G41–G47. Doi: 10.1149/2.0451508jes

Lemlikchi, W., Khaldi, S., Mecherri, M. O., Lounici, H., Drouiche, N. (2012) Degradation of Disperse Red 167 Azo Dye by Bipolar Electrocoagulation. *Sep. Sci. Technol*, **47**(11), 1682–1688. Doi: 10.1080/01496395.2011.647374

Martinez-Huitle, C.A., Brillas, E. (2009) Decontamination of wastewaters containing synthetic organic dyes by electrochemical

methods: A general review. *Appl. Catal. B: Environ*. 87 105–145. Doi: 10.1016/j.apcatb.2008.09.017

Matteson, M.J., Dobson, R.L., Glenn, R.W., Kukunoor, N.S., Waits, W.H., Clayfield, E.J. (1995) Electrocoagulation and separation of aqueous suspensions of ultrafine particles. *Colloids Surf*, A, **104**(1), 101−109. Doi: 10.1016/0927-7757(95)03259-G

Meunier, N., Drogui, P., Montané, C., Hausler, R., Mercier, G., Blais, J. F. (2006) Comparison between electrocoagulation and chemical precipitation for metals removal from acidic soil leachate. *J. Hazard. Mater.* **137**(1), 581−590. Doi: 10.1016/j.jhazmat.2006.02.050

Panizza, M., Cerisola, G. (2006) Olive mill wastewater treatment by anodic oxidation with parallel plate electrodes. *Water Res*, **40**(6), 1179−1184. Doi: 10.1016/j.watres.2006.01.020

Paraskeva, C.A., Papadakis, V.G., Tsarouchi, E., Kanellopoulou, D.G., Koutsoukos, P.G. (2007) Membrane processing for olive mill wastewater fractionation. *Desalination*, 213 218−229. Doi: 10.1016/j.desal.2006.04.087

Sayadi, S., Zorgani, F., Ellouz, R. (1996) Decolorization of olive mill waste-waters by free and immobilized Phanerochaete chrysosporium cultures. *Appl. Biochem. Biotechnol*. **56**(3), 265−276. Doi:10.1007/BF02786957

Ün, Ü.T., Koparal, A.S., Ogutveren, U.B. (2009) Electrocoagulation of vegetable oil refinery wastewater using aluminum electrodes. *J. Environ. Manage*. **90**(1), 428−433. Doi: 10.1016/j.jenvman. 2007.11.007

Ün, Ü.T., Uğur, S., Koparal, A.S., Öğütveren, Ü.B. (2006) Electrocoagulation of olive mill wastewaters. *Sep. Purif. Technol*, **52**(1), 136−141. Doi: 10.1016/j.seppur.2006.03.029

Yahiaoui, O., Lounici, H., Abdi, N., Drouiche, N., Ghaffour, N., Pauss, A., Mameri, N. (2011) Treatment of olive mill wastewater by the combination of ultrafiltration and bipolar electrochemical reactor processes. *Chem. Eng. Process. Process Intensif*, **50**(1), 37−41. Doi: 10.1016/j.cep.2010.11.003

Zenjari, B., El Hajjouji, H., Ait Baddi, G., Bailly, J-R., Revel, J-C., Nejmeddine, A., Hafidi, M. (2006) Eliminating toxic compounds by composting olive mill wastewater-straw mixtures. *J Hazard Mater*, **138**(3), 433–437. Doi: 10.1016/j.jhazmat.2006.05.071